Global Sensitivity Analysis of the distributed hydrologic model ParFlow-CLM (V3.6.0)

Wei Qu[1*], Heye Bogena[2], Christoph Schüth[1], Harry Vereecken[2], Zongmei Li[3], Stephan Schulz[1]

[1]Institute of Applied Geosciences, Technische Universität Darmstadt, 64287 Darmstadt, Germany
5 [2]Agrosphere (IBG-3), Forschungszentrum Jülich GmbH, Jülich, 52425, Germany
[3]Department of Computer and Information Engineering, Xiamen University of Technology, China

Correspondence to: Wei Qu (wei.qu@geo.tu-darmstadt.de)

Abstract. The integrated distributed hydrological model ParFlow-CLM was used to predict water and energy transport between subsurface, land surface, and atmosphere for the Stettbach headwater catchment, Germany. Based on this model, a
10 global sensitivity analysis was performed using the Latin-Hypercube (LH) sampling strategy followed by the One-factor-At-a-Time (OAT) method to identify the most influential and interactive parameters affecting the main hydrologic processes. In total 12 parameters were evaluated including soil hydraulic properties, storage, Manning coefficient, leaf area index, stem area index, and aerodynamic resistance that characterize water and energy fluxes in soil and vegetation. In addition, the sensitivity analysis was also carried out for different slopes and meteorological conditions to test the transferability of the results to
15 regions with other topographies and climates. Our results show that the simulated energy fluxes, i.e. latent heat flux and sensible heat flux are sensitive to the parameters such as wilting point, leaf area index, and stem area index, especially for steep slope and subarctic climate conditions. The simulated soil evaporation, plant transpiration, infiltration, and runoff, are most sensitive to soil porosity, the van Genuchten parameter n representing the soil pore size distribution, soil wilting point, and leaf area index. The subsurface soil water storage and groundwater storage are most sensitive to soil porosity, while the
20 surface water storage was most sensitive to the soil roughness parameter. For the different slope and climate conditions, the rank order of input parameter sensitivity is consistent, but the magnitude of parameter sensitivity is very different. The strongest deviation in parameter sensitivity occurred for sensible heat flux under the different slope conditions as well as for transpiration under different climate conditions. Overall, this study provides an insight into the most important input parameters that control hydrological fluxes and how the simulated variables vary with the change in parameter values, which can improve our
25 understanding of the key processes in the model and help us to reduce the computational demands of completing multiple simulations of expensive domains.

1 Introduction

Ever growing water demands and changing climatic conditions cause increasing pressure on surface water and groundwater resources. A rigorous quantitative understanding of the interactions and feedback mechanisms in the hydrological systems is
30 therefore essential for a sound and sustainable water management, especially on a catchment scale (Blöschl et al., 2019; Jolly et al., 2008; Maxwell et al., 2015; Melsen and Guse, 2021; Sophocleous, 2002). This has created the need for integrated coupled

water flux modelling approaches that can assess the dynamics of surface water and groundwater resources as well as their interactions, e.g. for predicting the effects of future climatic changes on the hydrological systems, and to evaluate the effectiveness of adaptation measures in water management (Brunner et al., 2017; Butturini et al., 2002; Jencso et al., 2010).

35 Consequently, a growing number of open source and commercial distributed hydrological models with varying degrees of complexity have been developed and applied that also consider the feedback processes between soil, vegetation, and atmosphere, e.g. HydroGeoSphere (Cornelissen et al., 2014; 2016); MIKE-SHE (Graham and Butts, 2005); TerrSysMP (Gebler et al., 2017) and ParFlow-CLM (Fang et al., 2016; 2015). The choice of the modelling platform for a given problem is often based on subjective criteria, on appropriateness of the available database, or simply on model availability. However,

40 also inter-comparison studies of such models are available, e.g. Koch et al. (2016) applied HydroGeoSphere, MIKE-SHE, and ParFlow-CLM to a well-defined and small headwater catchment. They reported that all three models performed well in terms of discharge and accumulated water balance components, although ParFlow-CLM predicting more accurately the temporal and spatial dynamics of the water balance components at the scale of the small catchment. The rapid increase in computing power allows to apply models like ParFlow-CLM also to large catchments and over long time periods (Maxwell et al., 2015;

45 Kollet and Maxwell, 2008a; Wood et al., 2011).

Still, one of the most crucial points of all models is the quite large number of input parameters that can be defined and the complex underlying mathematical algorithms. Their sensitivities to the modelling results in space and time, as well as their combined effects, cannot be easily analysed. Thus, there is a strong need to identify the most relevant processes and parameters controlling hydrological behaviour, to target a subset of parameters to be included in more computationally intensive

50 sensitivity, uncertainty and parameter estimation analyses (Abdel-Khalik et al., 2013; Castaings et al., 2009; Devak and Dhanya, 2017). In addition, the identification of sensitive parameters should also help to reduce the danger of non-unique solutions, i.e. equifinality. This is especially important in basins where water management decisions are being made and where highly nonlinear-coupled hydrologic processes make it difficult to develop a predictive understanding of the hydrologic behavior of the system. A variety of formal sensitivity analysis approaches exist, such as elementary effects methods (Cropp

55 and Braddock, 2002; Morris, 1991), variance-based methods (Saltelli et al., 2010), Fourier amplitude sensitivity testing (Saltelli et al., 1999), and hybrid methods (Abdel-Khalik et al., 2013). The global method Latin-Hypercube-One-factor-at-A-Time (LH-OAT) strategy (van Griensven et al., 2006) enables parameter sensitivity analyses of computationally expensive models because of the considerably smaller number of model executions required to efficiently separate sensitive parameters from the insensitive ones.

60 The sensitivity of model parameter depends on climate and topography of the model domain, which may have strong implications for model calibration (Abily et al., 2016; Fernandez-Pato et al., 2016; Melsen and Guse, 2021). Recently, Melsen and Guse (2021) investigated the impact of climate change on parameter sensitivity for three hydrological models (SAC, VIC, and HBV) across 605 catchments in the United States. They reported that both for the mean of discharge and the timing of the discharge the sensitivity of snow parameters declines, while the sensitivity of evaporation parameters shows a tendency to

65 increase in the three investigated hydrological models within a plausible climate change rate. Fernandez-Pato et al. (2016)

applied a Horton/Green-Ampt model coupled with a 2D surface flow model to different slope conditions and found that the topography of the catchment strongly influences the calibration of infiltration parameters. Göhler et al. (2013) analysed the sensitivity of energy fluxes for land surface model (CLM, version 3.5) with the eigendecomposition method, they reported that it is important to implement specific physiological parameters for diverse crop species in order to accurately model heat and

70 matter fluxes.

The overall objective of this study is to use the global sensitivity analysis LH-OAT strategy to explore the parameter sensitivity of ParFlow-CLM, applied to a small catchment in southwestern Germany. The ParFlow-CLM model is a three-dimensional, finite-difference, parallel computing hydrological model that computes variably saturated surface-subsurface flow and surface-atmosphere energy exchange fluxes in complex real-world systems (Maxwell et al., 2015; Maxwell and Miller, 2005). It

75 couples the subsurface water flow model ParFlow (Maxwell, 2013, Kollet and Maxwell, 2006) with the Community Land Model-CLM (Dai et al., 2003; Oleson et al., 2008) to link water and energy fluxes among the subsurface, land surface, and atmosphere. We investigated the response of the energy- and water-related variables predicted by the model, e.g. latent heat flux, longwave radiation, sensible heat flux, evaporation, transpiration, infiltration, subsurface water storage, and runoff, to 12 representative hydraulic and vegetation parameters based on a two-year period covering both wet and dry seasons.

80 Furthermore, the effect of different climates and topographies on parameter sensitivity was investigated to test the transferability of the results to regions with other topographies and climates.

2 Methods

2.1 The ParFlow-CLM Model (v3.6.0)

ParFlow is an open-source fully integrated distributed hydrological model (Kollet and Maxwell, 2006; Maxwell, 2013), which

85 solves the 3D Richards Equation (Eq. 1) using a cell-centered finite difference scheme in space and a backward Euler scheme in time for variably saturated subsurface conditions and overland flow boundary. Surface flow simulations are described by the kinematic wave approximation of the continuity equation (Eq. 2) and flow-discharge relationships for vertical and horizontal direction are expressed by Manning's equation (Eq.3).

$$S_s S_\psi \frac{\partial \psi}{\partial t} + \varphi \frac{\partial S_\psi}{\partial t} = \nabla \cdot [K(\psi)\nabla(\psi - z)] + q_s \qquad \text{Eq. 1}$$

90

$$-K(\psi)\nabla(\psi_0 - z) = \frac{\partial \|\psi_0, 0\|}{\partial t} - \nabla \cdot \vec{\vartheta} \|\psi_0, 0\| - q_r \qquad \text{Eq. 2}$$

$$\vartheta_x = \frac{\sqrt{S_{f,x}}}{n} \psi_0^{2/3}; \quad \vartheta_y = \frac{\sqrt{S_{f,y}}}{n} \psi_0^{2/3} \qquad \text{Eq. 3}$$

where Ss is the specific storage coefficient [L^{-1}]; ψ is the pressure head of water [L]; Sψ and K(ψ) are the degree of saturation [-] and hydraulic conductivity [LT^{-1}], which are a function of pressure head defined by the van Genuchten model (1980); φ is the porosity [-]; z is depth below the land surface [L]; q$_s$ is a general source/sink term, which includes infiltration, evaporation

95 and transpiration [LT^{-1}]; ϑ is the depth averaged velocity vector of surface runoff [LT^{-1}]; q$_r$ represents rainfall and evaporative

fluxes [LT^{-1}]; $S_{f,x}$ and $S_{f,y}$ are the friction slopes in x and y direction [-]; n is the Manning's coefficient [TL$^{-1/3}$]; ψ_0 is the pressure head or water ponding depth at the land surface [L]; and the $\|\psi_0, 0\|$ operator is defined as the larger of the two quantifiers, ψ_0 and 0.

In ParFlow-CLM, the Community Land Model version 4.0 (CLM4.0, Dai et al., 2003) is included as a module within ParFlow over the top ten grid cells starting at the land surface and moving downward (Maxwell and Miller, 2005; Rihani et al., 2010). CLM4.0 is composed of a series of land surface modules that are called as a subroutine within the ParFlow integrated hydrologic model to compute energy and water fluxes (e.g., evaporation and transpiration) into and out of the land surface.

$$E_{gr} = -\beta \rho_a \mu_* q_* \qquad \qquad \text{Eq. 4}$$

$$E_{veg} = [R_{pp,dry} + L_w] L_{SAI} [\frac{\rho_a}{r_b} (q_{sat} - q_{af})] \qquad \text{Eq. 5}$$

For example, the CLM computes the bare ground surface evaporation according to Eq. 4 and evapotranspiration for vegetated land surface according to Eq. 5. where ß is the soil resistance factor [-], ρ_a is air density [ML^{-3}], μ_* is friction velocity [LT^{-1}], q_* is humidity scaling parameter [-], r_b is the air density boundary resistance factor [LT^{-1}], q_{sat} is saturated humidity at the land surface [-], q_{af} is the canopy humidity [-], $R_{pp,dry}$ is the transpiration depends on the dry fraction of the canopy [-], L_w is the fraction of foliage covered by water [-], L_{SAI} is the sum of the leaf and stem area indices [-]. A detailed description of the equations of ParFlow-CLM can be found in Jefferson et al. (2015) and Srivastava et al. (2014).

The soil water content simulated by ParFlow is passed to CLM, and the infiltration, evaporation, and root uptake fluxes simulated by CLM are passed back to ParFlow, where they are treated as water fluxes into or out of the model. This creates a fully integrated modelling approach that links overland and subsurface flow while providing an explicit representation of the groundwater table and all land surface processes forced by atmospheric data. Because the groundwater table is explicitly represented in these simulations, regions with a strong interaction between groundwater and the land surface energy balance (i.e. critical zones) can be identified (Kollet and Maxwell, 2008a; Kollet and Maxwell, 2008b).

2.2 The LH-OAT sensitivity analysis

The Latin-Hypercube One-factor-at-A-Time (LH-OAT) sampling strategy (van Griensven et al., 2006) performs Latin-Hypercube (LH) sampling (Stein, 1987) using the One-factor-at-A-Time (OAT) method (Cropp and Braddock, 2002) to reduce the computational cost required to propagate and understand the key sources of parameter sensitivity. First, N Latin hypercube sample points are taken for n intervals, and then each LH sample point is varied P times by changing each of the P parameters once, as in the OAT method. This is more efficient than LH, as the N intervals in the LH method require only a total of N*(P+1) runs. In this way, the computational effort for the sensitivity analyses of complex integrated models such as ParFlow-CLM is greatly reduced, as a much smaller number of model runs are required to identify the most sensitive model parameters.

After each model run, the change in output is attributed to the change in a single parameter, and the local effect at the sample point of each parameter is evaluated with the partial effect using Eq. 6. Consequently, the final effect (S_i) is calculated by averaging these partial effects in percentage of each loop for all LH points (N loops, Eq. 7). The magnitude of S_i indicates the

degree of parameter sensitivity and the sign of S_i signifies whether the output variables will increase or decrease with changes of the input parameters.

130

$$S_{i,j} = \left. \frac{100*[F(p_1,...,p_i*(1+f_i),...,p_p)-F(p_1,...p_i,...,p_p)]}{F(p_1,...,p_i*(1+f_i),...,p_p)+F(p_1,...p_i,...,p_p)} \middle/ f_i \right. \qquad \text{Eq.6}$$

$$S_i = \frac{1}{N}\sum S_{i,j} \qquad \text{Eq.7}$$

Where F(•) refers to the model functions, f_i is the fraction by which the parameter p_i is changed and j refers to a LH point.

2.3 Design of the sensitivity analysis

In the following, we present the Stettbach catchment, which was used as the model domain for the ParFlow-CLM simulations,
135   and the concept of sensitivity analysis including its transferability to different slope and climate conditions. The Stettach catchment was chosen for this study because of its low human impact and because it has been intensively investigated in a number of unpublished post and undergraduate studies at the TU Darmstadt.

2.3.1 Characteristics of the Stettbach catchment

The headwater catchment of the Stettbach is located in the Odenwald low mountain range in Germany and covers an area of
140   about 4 km². It represents a typical mountainous catchment, mainly covered by forests and pasture (Figure 1). It is instrumented with three discharge stations (since 2020) and one weather station (since 2018). It ranges from 184 to 445 m a.s.l. with an average slope of about 20%. The dominant soil texture is silty loam. The mean annual precipitation based on data from the last 35 years is 870 mm, ranging from about 535 mm (2018) in the driest year to 1200 mm (1987) in the wettest year during the recording period. The mean annual temperature of the catchment is about 11 °C with January being the coldest and July the
145   warmest month of the year.
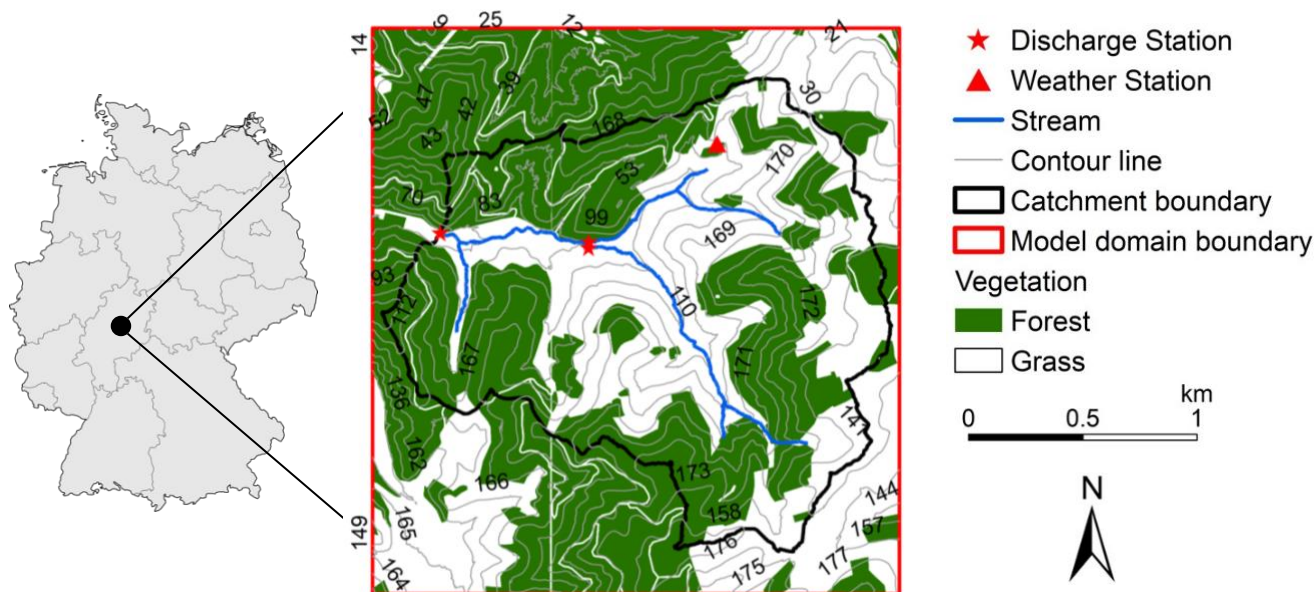
Figure 1. Map of the Stettbach model domain with catchment boundary, topography and spatial distribution of vegetation

2.3.2 Observations in Stettbach catchment

For this study, precipitation, air temperature, solar radiation, long wave radiation, wind speed and direction, atmospheric
150   pressure, and humidity at hourly resolution were obtained from the weather station within the catchment (Figure 1). Wind
speed was obtained with an ultra-sonic anemometer at 1.5 m above surface (WINDSONIC1, Campbell Scientific). Air
temperature and humidity were measured with a combined probe (CS215, Campbell Scientific) between 1.5 m and 2 m height
above the ground surface. Air pressure was measured with barometric pressure sensor (CS106, Campbell Scientific) at the
same height of air temperature and humidity. Incoming short- and long-wave radiation were determined using a net radiometer
155   (NR-LITE2, Campbell Scientific). Precipitation was measured by a tipping bucket rain gauge (52202, Campbell Scientific).
Data of all instruments including diagnostic data were recorded with a data logger (CR800, Campbell Scientific) with a one-
hour recording interval. Missing data were filled in with data from the weather stations Latertal operated by the German
Weather Service, which are located about 6 km southeast and 19 km north of the study area, respectively. The hourly time
series meteorological forcing data are presented in Figure A1.

160   2.3.3 Description of the ParFlow-CLM model for Stettbach catchment

The model domain for the Stettbach catchment was set to 2900×2700 m with a depth of 10 m with a horizontal grid resolution
of 50 m and a vertical discretization of 0.2 m using the terrain following grid (TFG) option. For this, a digital elevation model
with a resolution of 1 m (DGM1) for the catchment was obtained from the Hessian Agency for Land Management and
Geoinformation and converted to a 50 m grid. Overland flow boundary condition was specified at the land surface, no-flow

boundary condition was specified for the bottom of the model domain and hydrostatic equilibrium condition was chosen for the lateral boundaries, i.e., the surface water divide. Subsurface hydraulic parameters were assumed to be homogenous and isotropic, and were estimated by the pedotransfer function of Rosetta (Schapp et al., 2001) using soil texture information measured in the lab. The hydraulic properties of the bedrock were estimated with the information from the Hessian Agency for Nature Conservation, Environment and Geology (HLNUG). A model spin-up is important to provide a realistic initial condition for the modelling (Ajami et al., 2014; Seck et al., 2015). In this study, a time series of atmospheric forcing data (1985-2016) was used for spinning up the ParFlow-CLM model until the difference between the beginning and ending of water and energy storage drops below a threshold value. The spatial distribution of pressure head resulting from this spin-up process was used to initialize all simulation runs of this study.

2.4 Selected parameters for the sensitivity analysis

A selected set of model parameters (as described in Table 1) have been used in the sensitivity analysis in order to capture the major processes of the ParFlow-CLM. Due to the high computational cost of the Parflow-CLM model, a reduced set of vegetation parameters was selected related to the CLM land cover type mixed forest. All the other CLM input parameters related to energy budget calculations were fixed to their default values (Jefferson et al., 2015; Srivastava et al., 2014). Thus, a total number of 12 parameters and 30 LHs were considered in the global sensitivity analysis (Wang, et al., 2019), resulting a total number of 390 model runs with different parameter combinations based on the parameter ranges summarized in Table 1. The range of these parameters used in our study were based on ranges of values given in the published literature (Jefferson et al., 2015; Jefferson and Maxwell, 2015; Jefferson et al., 2017; Schaap et al., 2001; Srivastava et al., 2014) or estimated from our field work. The simulations for the global sensitivity analysis were run on the Lichtenberg II high-performance computer of the TU Darmstadt with a real peak performance of over 3148 PFlop/s and a total of 257 TByte RAM. The model execution time depended on the difficulty level posed by combination of parameter values and it ranged from 2 hours to 6 days for each model run.

Table 1 ParFlow-CLM parameters included in Global Sensitivity Analysis by the LH-OAT method.

	Parameter name	Abbreviation	Distribution[a]	Unit
Parflow Parameters	1 Residual saturation	Sres	U(0, 0.2)	-
	2 Porosity	$\varnothing$	U(0.3, 0.7)	-
	3 van-Genuchten α	vG_α	U(0.04, 12.8)	m^{-1}
	4 van-Genuchten n	vG_n	U(1.4, 4.8)	-
	5 Hydraulic conductivity	K_s	U(1.00E-3, 3)	mh^{-1}
	6 Manning's n	n	U(1.00E-4, 1)	hm$^{-1/3}$
	7 Specific storage	Ss	U(1.00E-8, 0.01)	m^{-1}

CLM parameters	8 Field capacity	fc	U(0.1,0.5)	-
	9 Wilting point	wp	U(0.1, 0.3)	-
	10 Leaf area index (Maximum)	LAI	U(3, 9)	-
	11 Stem area index	SAI	U(1, 3)	-
	12 Aerodynamic roughness length	z0	U(0.1, 1.2)	m

[a] U(min, max), uniform probability distribution in the range (minimum, maximum).

2.5 Effects of topography and climate on the sensitivity analysis

Furthermore, we aimed to examine to what extent the results of our sensitivity analysis can be transferred to other areas. Therefore, we have also performed the sensitivity analysis for model domains with modified topography and climatology from other regions.

2.5.1 Topography effects

To determine the effects of topography on the parameter sensitivity, we applied two modifications to the original slope from Stettbach catchment, i.e., low slopes (50% of the slope in Stettbach catchment) and high slopes (130% of the slope in Stettbach catchment; Figure 2), with the model setup otherwise remaining unchanged. The slope of the model was calculated from DEM with the watershed analysis tool in ArcGIS in order to get a hydrologically consistent slope for the model.
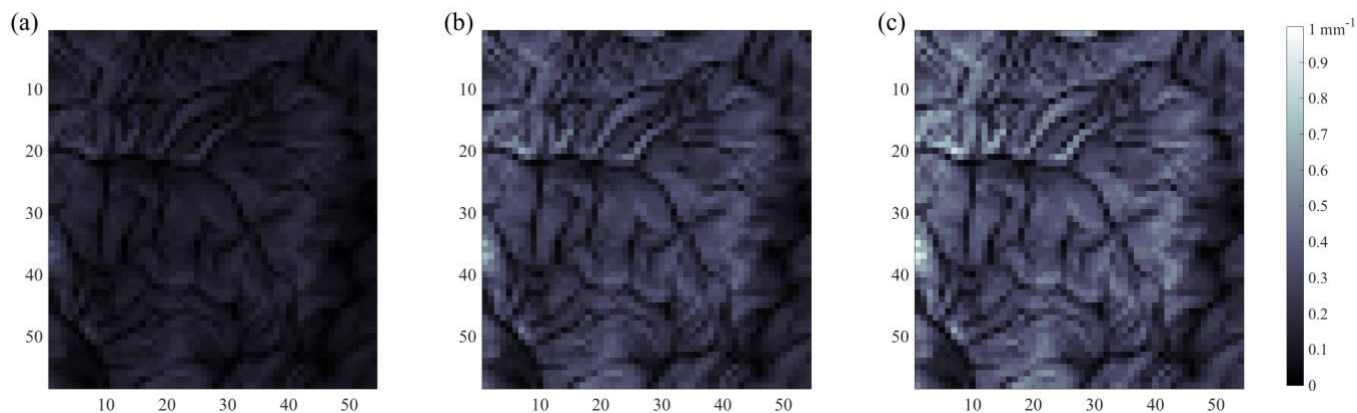
Figure 2. The topographies of the three different slope variants (a) low slopes, (b) medium slopes, (c) high slopes used for the sensitivity analysis.

2.5.2 Climate effects

In order to analyze the effect of climate on the parameter sensitivity we used meteorological datasets from three different climate zones: (i) temperate climate (Stettbach catchment, Germany), (ii) semi-arid climate (Barcelona, Spain), and (iii) subarctic climate (Lemmenjoen Kansallispuisto, Finland; Kottek et al., 2006). Eight atmospheric variables (shortwave

radiation, longwave radiation, precipitation rate, air temperature, east-west and north-south wind speeds, atmospheric pressure and specific humidity) are required for the computation of the water and energy flux in ParFlow-CLM. The two and half years (from 2016-07-01 to 2018-12-31) hourly meteorological forcing data for Barcelona and Lemmenjoen Kansallispuisto were derived from the ERA5 dataset (ECMWF Reanalysis v5; Bell et al., 2021; Hersbach et al., 2020) and presented in Figure A2

210 and Figure A3. The diagrams about the monthly temperature, precipitation, and evaporation of each catchment plotted in Figure 3 provided an overview (expressed in air temperature and precipitation) among the three climate conditions. The other model settings for the three different climatic conditions were the same as for the Stettbach catchment.
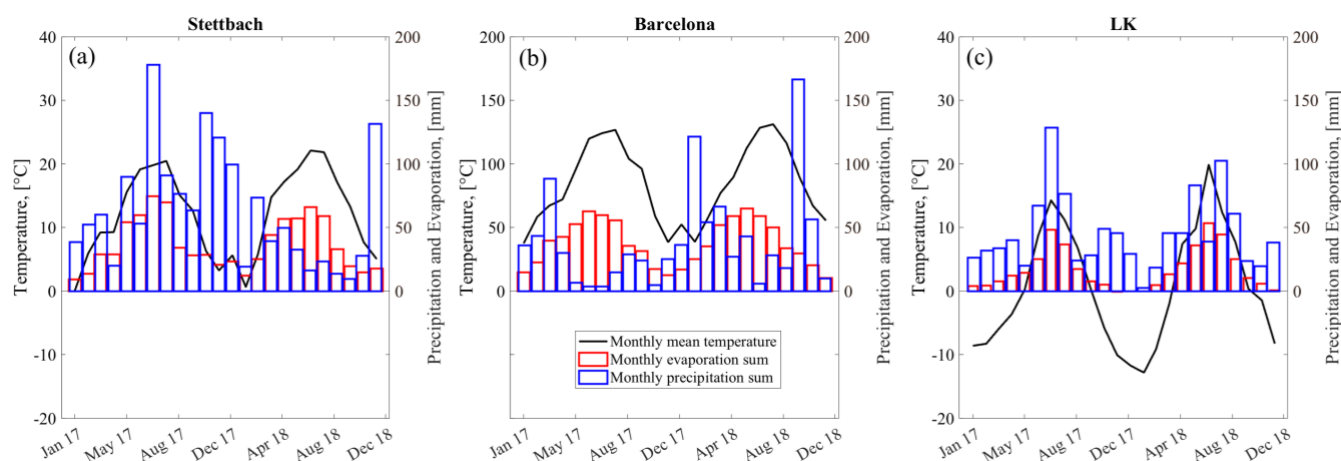
Figure 3. Monthly temperature, precipitation, and total actual evaporation of each climate station, i.e. Stettbach (Odenwald,
215 **German), Barcelona (Spain), and Lemmenjoen Kansallispuisto (LK, located in the Lemmenjoki national park in Finland); black line is monthly mean air temperature, blue column is monthly cumulative precipitation, and red column is month cumulative evaporation in 2017 and 2018.**

3 Results and Discussions

3.1 Model performance in Stettbach catchment

220 Before conducting the sensitivity study, we tested whether ParFlow-CLM is able to adequately predict the hydrological fluxes of the Stettbach catchment. Since a fully automatic calibration of the model parameters is practically not feasible due to the complicated hydrological model, we performed the simulations using parameters created by Latin-Hypercube method and selected the model run with the best agreement with the observed discharge. The simulation time period was extended to January 2022 in order to compare our simulated and observed runoff data at the outlet of the catchment. The best simulated

225 model was plotted in Figure 4. Simulated and observed runoff agree in their temporal pattern, showing a period with high flow in winter and low flow conditions in summer. The coefficient of determination (R^2), root mean square error, and Nash–Sutcliffe model efficiency coefficient (NSE) between our simulated and observed runoff are 0.92, 22.34 m^3h^{-1}, and 0.79, respectively.

This indicates that the ParFlow-CLM model can capture the main hydrological dynamics of the Stettbach catchment reasonably well.
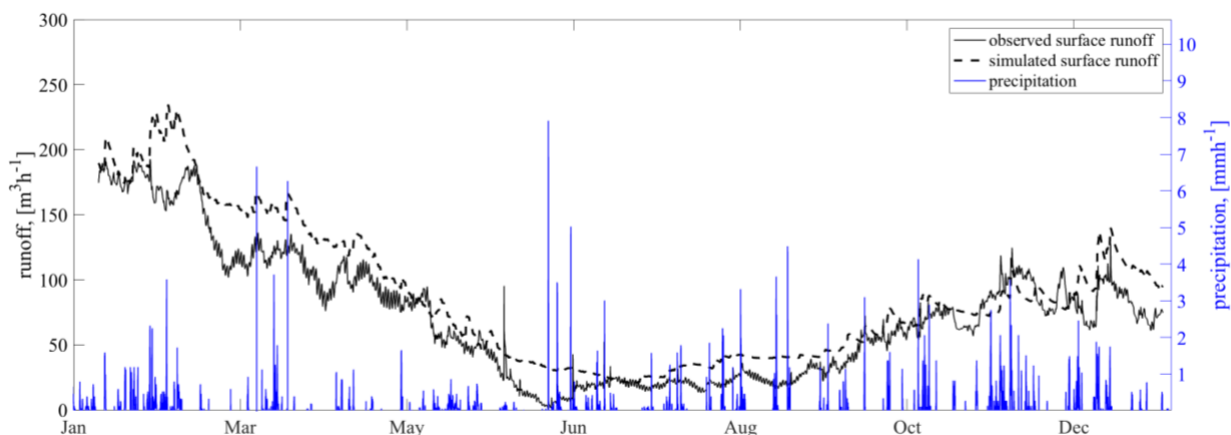
230

Figure 4. Simulated and observed hourly runoff of the Stettbach catchment from 01.01. 2021 to 31.01.2022.

Water balance is an important component of catchment studies, which describes the partitioning of the incoming precipitation into discharge, storage and evapotranspiration. Figure 5 provides an overview of the water balance components including simulated and observed discharge, evaporation, transpiration, and precipitation. It can be seen that ParFlow-CLM slightly

235 overestimated the discharge by about 60 mm. This indicates that there are still inaccuracies in the model parameters resulting from the fact that we only consider a spatial homogeneous soil and vegetation parameters. Therefore, in a future study, spatial heterogeneous soil and vegetation properties in the Stettbach catchment will be applied to better estimate the runoff and other variables of ParFlow-CLM. However, as this study focuses on investigating the sensitivity of the ParFlow-CLM model parameters, we believe that these parameter inaccuracies do not affect our results.
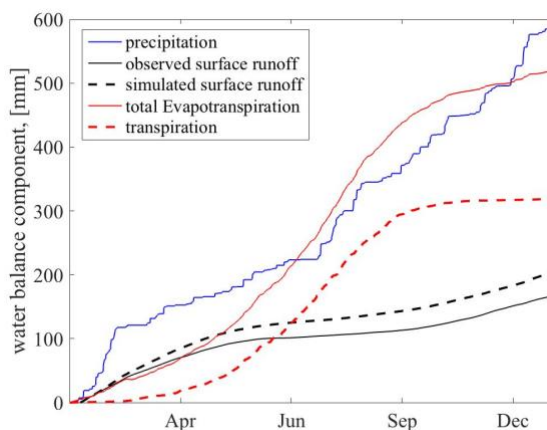
240

Figure 5. Simulated annual cumulative water balance components precipitation, total evapotranspiration, transpiration, observed surface runoff, and simulated surface runoff from 01.01. 2021 to 31.01.2022.

3.2 Sensitivity analysis of Stettbach catchment

The average partial effects (in percentage) for all the 12 parameters of all Latin Hypercube loops are listed in Table 2, it shows
245 the most sensitive and insensitive parameters with respect to selected output variables. The partial effects with larger magnitudes imply that the corresponding parameters cause more change in the model variables than those with small partial effects. The sign of partial effects indicates whether the model variables will increase or decrease with changes in the model parameters. For example, since the partial effect of leaf area index (LAI) on latent heat was positive, this indicates that latent heat will increase with increasing LAI. On the other hand, since the partial effect of the van Genuchten parameter n (vG_n)
250 and the wilting point (wp) was negative for latent heat, the latent heat will decrease with the increase of these parameters. These relationships are consistent with physical intuition. For instance, a higher LAI favours transpiration, resulting in more latent heat.

The extent to which the model variables responded to parameter changes varied greatly. For instance, the partial effects of longwave radiation (lwrad) and surface soil temperature (t_soil) were close to zero indicating that these variables are not very
255 sensitive. The partial effects of the 12 parameters were not consistent between different energy fluxes (i.e. latent heat flux, sensible heat flux, and ground heat flux), multiple parameters were found sensitive depended on the type of energy. Such as sensible heat flux was most sensitive to the parameter of leaf area index (LAI), the van Genuchten parameter n (vG_n), aerodynamic resistance (z0), and wilting point (wp); and latent heat was most influenced by the wilting point (wp), leaf area index (LAI); however, the ground heat was only sensitive to vG_n. From a physical perspective, the soil moisture may have a
260 strong effect on ground heat flux, because it influences both ground temperature as well as the amount of water available for evaporation and transpiration. The parameters controlling unsaturated zone flow process played an important role in controlling evapotranspiration loss. Such as evaporation (E) and transpiration (T) were highly sensible to the change of wp and vG_n, followed by the vegetative property of LAI. Thus, ET is more sensitive to soil/geologic properties than vegetative properties. Furthermore, the saturated hydraulic conductivity (K_s) had a negative impact on the model variables subsurface water storage
265 (ssw), groundwater storage (gw), surface water storage (sw), runoff and surface saturation level (ss), while porosity ($\emptyset$) showed positive effects on these model variables. Parameter K_s and $\emptyset$ have great influence on the availability of surface and subsurface water storage for rainfall, which in turn affect the amount of water contributing to streamflow and recharge potential for groundwater.

Table 2. The partial effect (in percentage, %) of the ParFlow-CLM parameters (listed in Table 1) for different model variables on
270 **the basis of a two-year simulation of the Stettbach catchment, the parameters with high partial effects to different variables were marked in grey.**

	Sres	$\emptyset$	vG_α	vG_n	Ks	N	Ss	fc	wp	LAI	SAI	z0
lh[1]	5.29	2.09	-4.25	-9.60	-3.53	0.04	0.03	-2.87	-10.32	10.04	-1.72	4.83
lwrad[2]	0.11	0.02	-0.06	-0.17	-0.06	0.00	0.00	0.04	-0.32	-0.10	0.00	0.11
sh[3]	-6.91	-4.27	9.75	23.83	5.34	-0.09	-0.29	4.60	12.64	-43.54	14.77	-21.77

grnd[4]	3.09	-3.54	-8.47	-12.20	-1.90	0.07	0.15	0.99	3.92	-2.52	0.84	-1.80
E[5]	5.41	1.98	-4.34	-9.90	-3.43	0.03	0.03	-2.83	-10.65	10.15	-1.54	4.72
T[6]	12.80	4.29	-7.48	-17.72	-9.21	0.13	-0.01	-7.34	-26.19	16.24	-9.90	-2.25
infl[7]	0.06	-0.55	1.14	3.04	0.65	-0.02	-0.03	-0.12	0.30	-0.93	-1.02	-3.97
swe[8]	-3.06	1.25	4.66	11.38	2.69	0.02	-0.05	-0.12	6.92	-4.44	-0.45	-18.39
t_soil[9]	0.03	0.00	0.00	0.01	0.00	0.00	0.00	0.01	-0.07	-0.04	-0.02	0.00
ssw[10]	-0.26	30.58	-1.70	-10.35	-7.95	-0.96	-0.08	-2.12	3.83	1.32	2.92	-3.00
gw[11]	-6.16	35.90	-1.35	1.49	-18.34	-2.07	1.84	-5.71	7.52	3.71	6.95	-7.17
sw[12]	-12.42	15	-10.97	6.05	-17.24	24.79	2.53	-10.07	13.97	3.65	13.91	-14.65
runoff[13]	-13.17	15.92	-17.63	8.64	-7.10	-7.76	2.57	-10.25	14.99	1.95	15	-16.28
SS[14]	4.38	4.91	-4.96	-28.08	-12.06	-0.78	0.53	-1.78	4.06	0.26	3.07	-3.06

[1]lh: latent heat flux [Wm^{-2}]; [2]lwrad: outgoing longwave radiation [Wm^{-2}]; [3]sh: sensible heat flux [Wm^{-2}]; [4]grnd: ground heat flux [Wm^{-2}]; [5]E: evaporation [mmhour^{-1}]; [6]T: vegetation transpiration [mmhour^{-1}]; [7]Infl: soil infiltration [mmhour^{-1}]; [8]swe: snow water equivalent [mm]; [9]t_soil: surface soil temperature [K]; [10]SSW: subsurface water storage [m^3]; [11]gw: groundwater storage[m^3]; [12]sw: surface water storage[m^3]; [13]runoff: surface water runoff [m^3]; 14 ss: surface saturation degree [-].

3.3 Sensitivity analysis for different slopes

The partial effects of the parameter sensitivity for ParFlow-CLM on the basis of a two-year simulation (from 01.01.2017 to 31.12.2018) for different slope conditions are presented in Figure 6. The slope effects on the output variable of longwave radiation (lwrad) and surface soil temperature (t_soil) were very low, indicating that these two model variables are only slightly dependent on the topography of the catchment. The sign of the partial effects of the different parameters were the same for different slope conditions, except in case of LAI for sensible heat flux, which indicates that the topography will not affect the increase or decrease of most output variables when the input parameters are changed. However, the magnitudes of the partial effects showed different behavior for different slope conditions, especially for latent heat (lh), ground heat flux (grnd), evaporation (E), transpiration (T), infiltration (infl), snow water equivalent (swe), surface water storage (sw), and runoff. Moreover, the sensitivity of soil hydraulic parameters did not significant change for the different slope conditions. However, the sensitivity of vegetation parameters, especially wilting point (wp), leaf area index (LAI), and stem area index (SAI) showed a clear difference between high slope and the other two slope (medium and low) conditions. The largest variation in parameter sensitivity was found for the sensible heat flux among the three different slope conditions, more specifically, the partial effect for the parameters wp, LAI, and SAI was much higher for the high slope condition compared to the low and medium slope conditions.
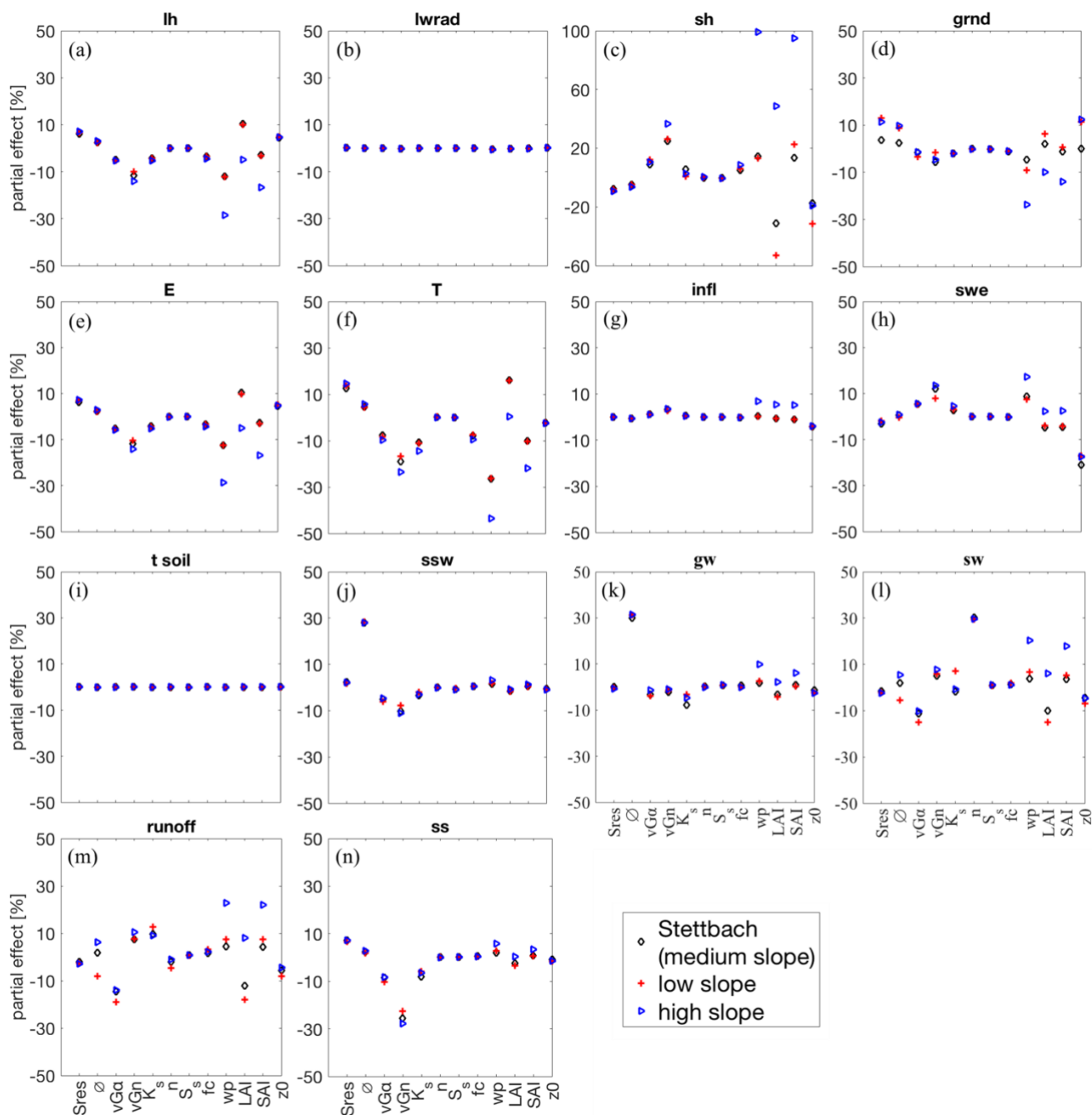
Figure 6. Slope effect on the sensitivity analysis for the different slope variants (low slope: 50% of the slope in Stettbach, high slope: 130% percentage of the slope in Stettbach) for the ParFlow-CLM output variables listed in Table 2. The X-axes of the subplots show the 12 Parflow-CLM parameters also listed in Table 1, and the Y-axes show the partial effect in percent.

3.4 Sensitivity analysis for different climatic conditions

Figure 7 shows how the parameter sensitivity of the 12 relevant parameters of the ParFlow-CLM model changes for the predicted energy- and water-related variables under the three different climatic conditions from 01.01.2017 to 31.12.2018. The model variables outgoing longwave radiation (lwrad) and soil temperature (t_soil) showed no variations to the parameters in different climate conditions, as both variables have very low sensitivity to changes in the model parameters in general. By introducing different climatic conditions, there was no change in the sign of the partial effects of the different parameters. However, the magnitude of the partial effect showed significant different for certain variables, i.e., latent heat (lh), ground heat flux (grnd), evaporation (E), transpiration (T), snow water equivalent (swe), surface water storage (sw), and runoff. In addition, transpiration was strongly influenced by the different climatic conditions, being more sensitive to LAI especially under cold climatic conditions than under the other two climatic conditions. The transpiration rate showed a markedly higher parameter sensitivity for the model parameters porosity, van Genuchten parameters α and n, saturated hydraulic conductivity and LAI under cold climate conditions compared to those under warm and relatively hot climate conditions. Differences in parameter sensitivity for transpiration in different climate conditions may primarily due to atmospheric forcing since vegetation is likely

not   limited   by   water   due   to   high   water   tables   in   the   catchment.
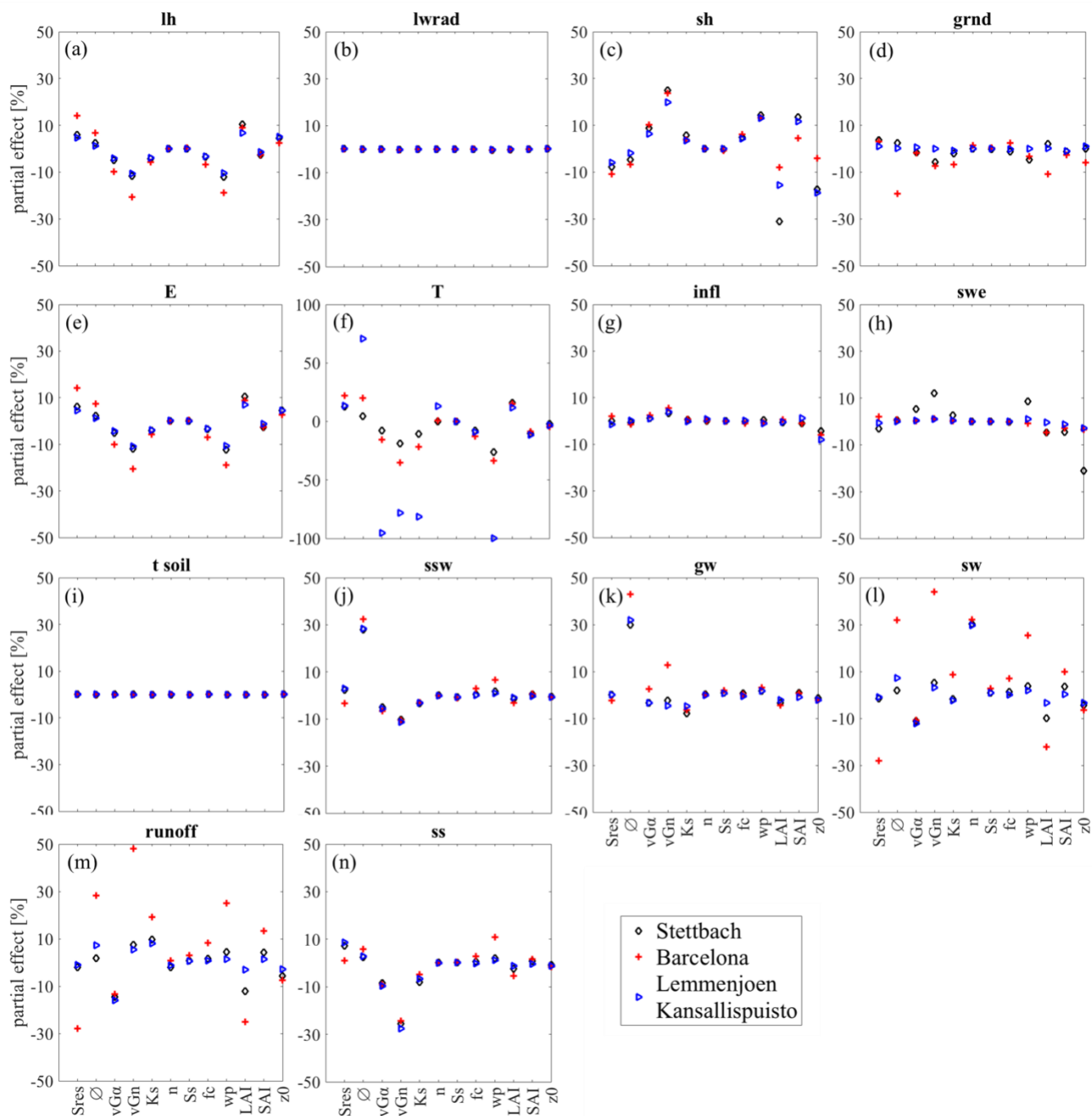
Figure 7. Climate effect on the sensitivity analysis for Stettbach (in Germany), Barcelona (in Spania), and Lemmenjoen Kansalispuisto (in Finland) for the ParFlow-CLM output variables listed in Table 2. The X-axes of the subplots show the 12 Parflow-CLM parameters also listed in Table 1, and the Y-axes show the partial effect in percent.

4 Conclusions

We applied the hydrological model ParFlow-CLM for a two-year simulation of the energy and water balance in the Stettbach
315 catchment in Germany and used a global sensitivity analysis, based on LH-OAT, for twelve selected model parameters. In
addition to the actual temperate climate scenario in the Stettbach catchment, we used meteorological datasets representing a
semi-arid climate, and a subarctic climate. We also modified the topography of the catchment resulting in lower slopes (50%
of actual slopes) and higher slopes (130% of actual slopes). With this, the general validity of the outcome of our sensitivity
analyses was analyzed and therefore the transferability to other catchments.

320 We found that the general patterns of the parameter sensitivities were consistent for the different climatic conditions, as well
as for the different terrain slopes. However, for some parameters a significantly larger span of the sensitivities in the different
scenarios was observed, especially for vegetation parameters on sensible heat flux in the higher slope scenario, and for
hydraulic parameters on transpiration rates in subarctic climatic conditions. In general, the variables related to energy fluxes
are more sensitive to vegetation properties as well as the van Genuchten parameter n, and the variables related to water fluxes
325 are more sensitive to both hydraulic and vegetation properties. We also found that some variables, i.e. the longwave radiation
and surface soil temperature, were not sensitive for all parameters.

It becomes more important to evaluate the sensitivity and behavior of model output such as energy and water fluxes for the
distributed hydrology model. The consistency of our results, especially as we applied different scenarios, may provide guidance
on the relative importance of the considered model parameters in setting up a simple and computationally cheaper domain
330 which can potentially be used to provide insight into the complex domains. In addition, the sensitivity results can be used to
support and complement a model upscaling process by providing insights on which parameter should be included in a more
comprehensive spatial-variable estimation.

5 Code and data availability

The exact version of the ParFlow-CLM (V3.6.0) model used to produce the results used in this paper is archived on Zenodo
335 (https://doi.org/10.5281/zenodo.4639761). The climate forcing data, model input files, parameter setup as well as scripts for
the analysing process for this study can be download from Zenodo (https://doi.org/10.5281/zenodo.6553492) and also upon
request from the corresponding author.

Acknowledgements

This research had been supported by the Deusche Forschungsgemeindschaft (DFG, Project Number: 459684982). The authors
340 gratefully acknowledge the hardware and software supported by the Lichtenberg High Performance Computer at Technische
Universität Darmstadt.

Appendix

Eight atmospheric variables (shortwave radiation, longwave radiation, precipitation rate, air temperature, east-west and north-south wind speeds, atmospheric pressure and specific humidity) are required in the computation of the water and energy flux

345 for ParFlow-CLM. The two and half years (from 01.07.2016 to 31.12.2018) hourly meteorological forcing data were derived from the climate station for Stettbach catchment and from ERA5 for Barcelona (in Spain, Figure A2), and Lemmenjoen Kansalispuisto (in Finland, Figure A3). Hourly time series meteorological forcing data of ParFlow-CLM were presented here. The mean annual precipitation in Stettbach is 870 mm, ranging from about 535 mm (2018) in the driest year to 1200 mm (1987) in the wettest year. The mean annual precipitation in Barcelona is 381 mm, ranging from about 236 mm (2015) in the

350 driest year to 632 mm (2018) in the wettest year. The mean annual precipitation in Lemmenjoen Kansallispuisto is 549 mm, ranging from about 418 mm (2015) in the driest year to 719 mm (2018) in the wettest year. Subsequently, the mean annual air temperatures are 11 °C in Stettbach, 16 °C in Barcelona, and 1 °C in Lemmenjoen Kansallispuisto, respectively.
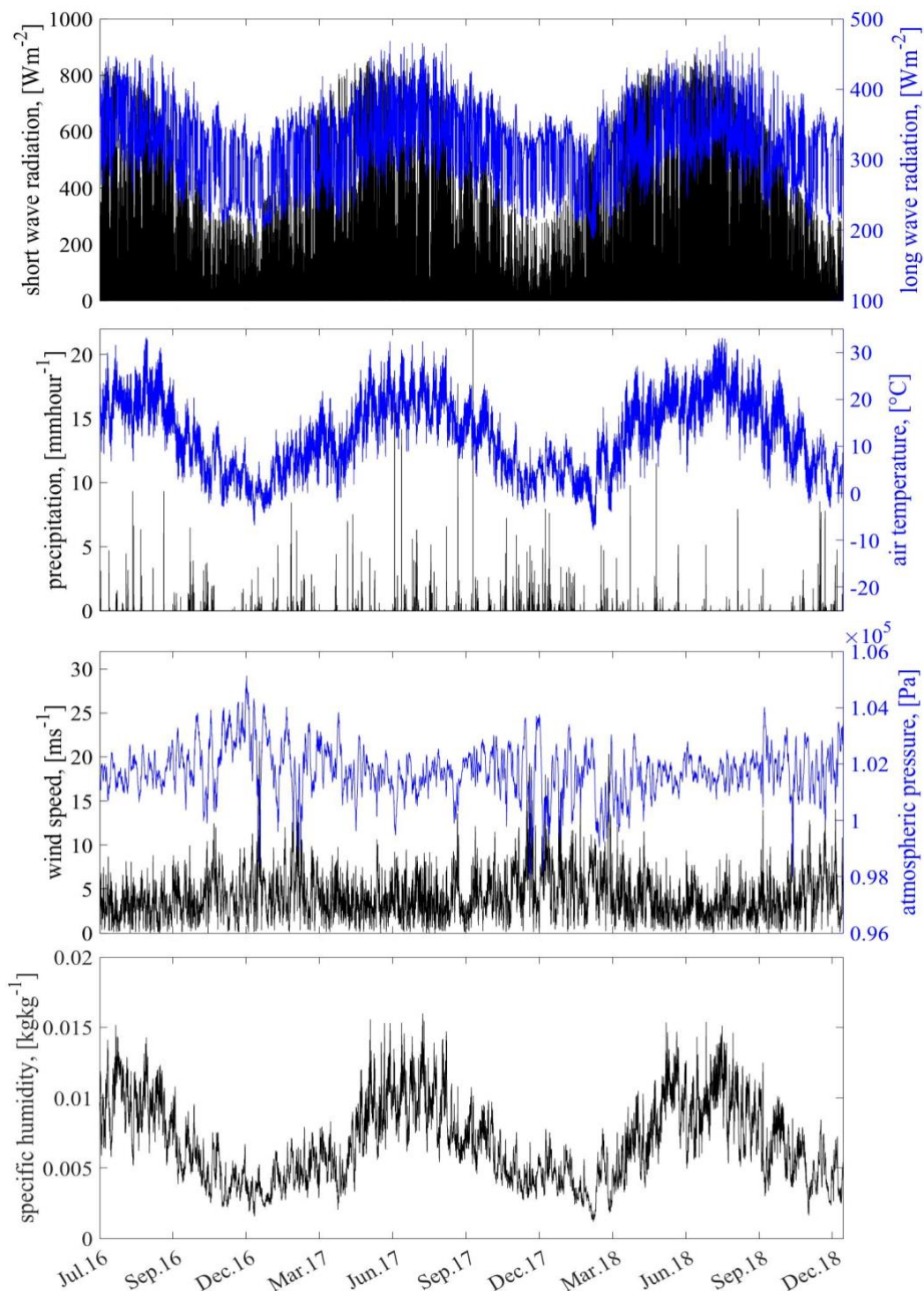
Figure A1. Hourly incoming shortwave (SW) and longwave (LW) radiation, precipitation, air temperature, wind speed, atmospheric pressure, and specific humidity used as meteorology forcing for the CLM model for the period 01.07.2016 – 31.12.2018 in Stettbach catchment (in Germany).

355
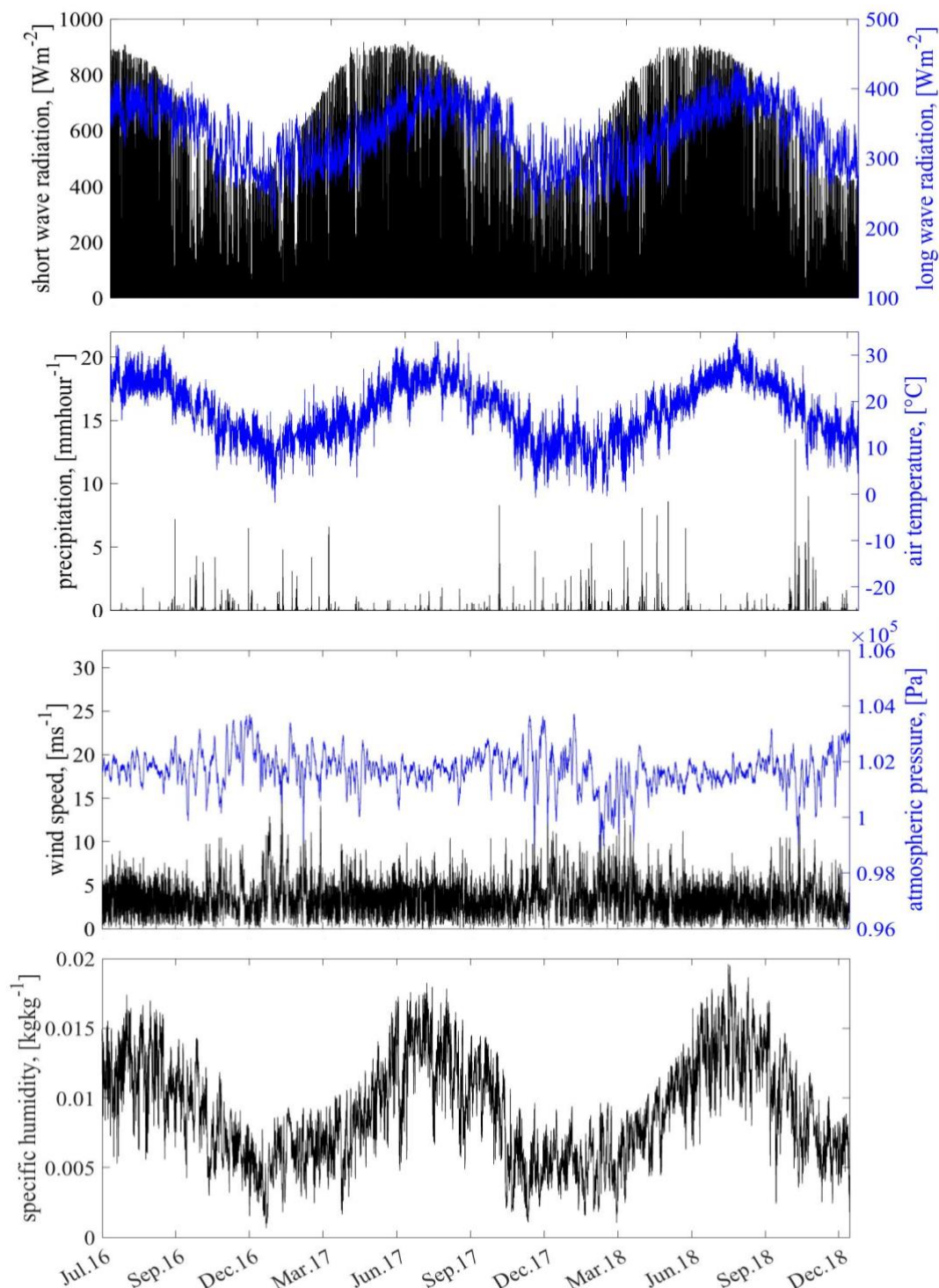
Figure A2. Hourly incoming shortwave (SW) and longwave (LW) radiation, precipitation, air temperature, wind speed, atmospheric pressure, and specific humidity used as meteorology forcing for the CLM model for the period 01.07.2016 – 31.12.2018 in Barcelona (in Spain).
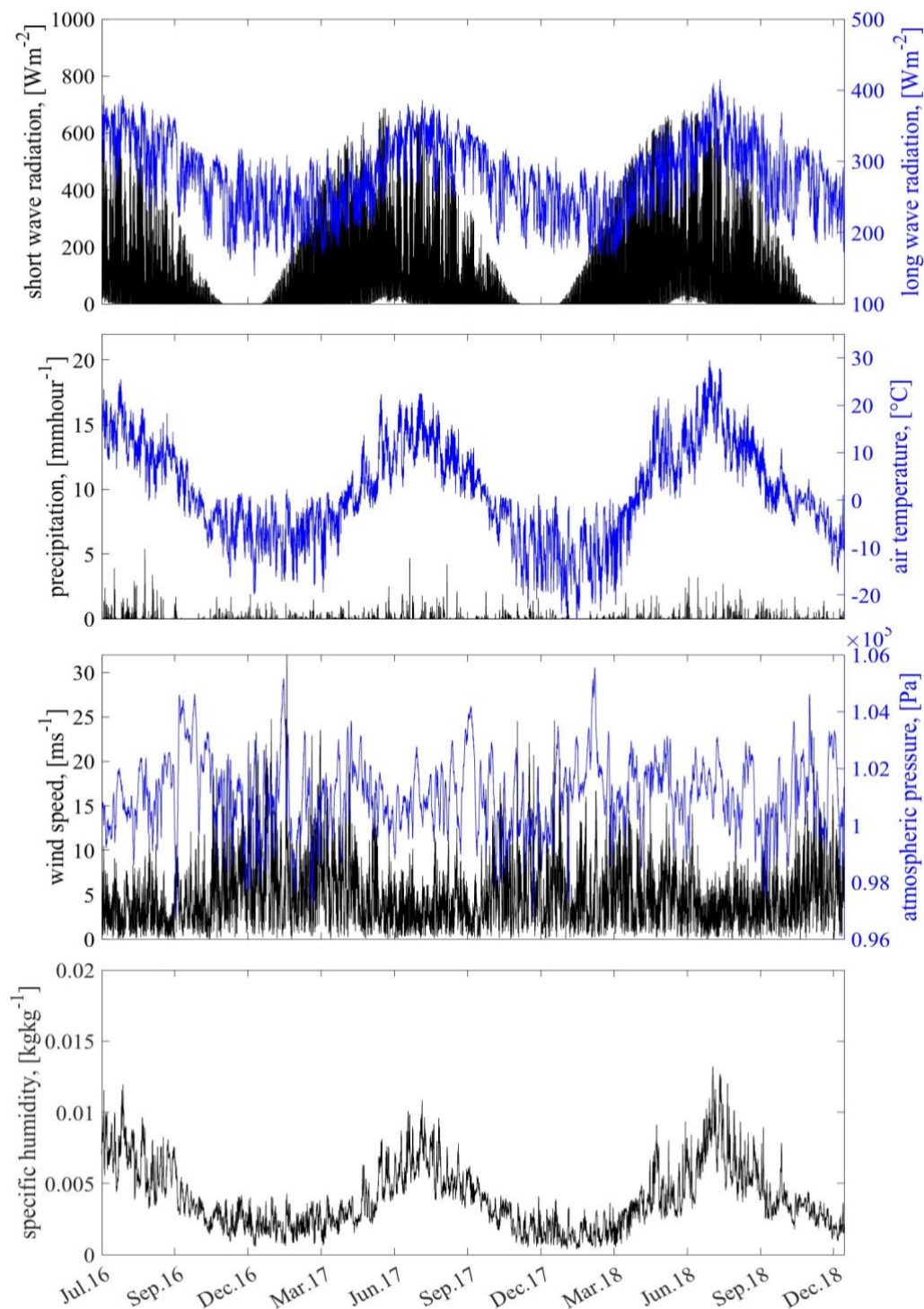
Figure A3. Hourly incoming shortwave (SW) and longwave (LW) radiation, precipitation, air temperature, wind speed, atmospheric pressure, and specific humidity used as meteorology forcing for the CLM model for the period 01.07.2016 – 31.12.2018 in Lemmenjoen Kansalispuisto (in Finland).

References

Abdel-Khalik, H.S., Bang, Y., et al. 2013. Overview of hybrid subspace methods for uncertainty quantification, sensitivity analysis. Ann Nucl Energy 52, 28-46.

365 Abily, M., Bertrand, N., et al. 2016. Spatial Global Sensitivity Analysis of High Resolution classified topographic data use in 2D urban flood modelling. Environmental Modelling & Software 77, 183-195.

Ajami, H., McCabe, M.F., et al. 2014. Assessing the impact of model spin-up on surface water-groundwater interactions using an integrated hydrologic model. Water Resour Res 50(3), 2636-2656.

Bell, B., Hersbach, H., et al. 2021. The ERA5 global reanalysis: Preliminary extension to 1950. Quarterly Journal of the 370 Royal Meteorological Society 147(741), 4186-4227.

Blöschl, G., Bierkens M., et al. (2019). "Twenty-three unsolved problems in hydrology (UPH) - a community perspective." Hydrological Sciences Journal 64(10): 1141-1158.

Brunner, P., Therrien, R., et al. 2017. Advances in understanding river-groundwater interactions. Rev Geophys 55(3), 818-854.

375 Butturini, A., Bernal, S., et al. 2002. The influence of riparian-hyporheic zone on the hydrological responses in an intermittent stream. Hydrol Earth Syst Sc 6(3), 515-525.

Castaings, W., Dartus, D., et al. 2009. Sensitivity analysis and parameter estimation for distributed hydrological modeling: potential of variational methods. Hydrol Earth Syst Sc 13(4), 503-517.

Cornelissen, T., B. Diekkrüger, and H.R. Bogena. 2014. Significance of scale and lower boundary condition in the 3D 380 simulation of hydrological processes and soil moisture variability in a forested headwater catchment. J. Hydrol. 516, 140-153. doi:10.1016/j.jhydrol.2014.01.060.

Cornelissen, T., B. Diekkrüger, and H.R. Bogena. 2016. Using High-Resolution Data to Test Parameter Sensitivity of the Distributed Hydrological Model HydroGeoSphere. Water 8(5), 202. doi:10.3390/w8050202.

Cropp, R.A. and Braddock, R.D. 2002. The New Morris Method: an efficient second-order screening method. Reliab Eng 385 Syst Safe 78(1), 77-83.

Dai, Y.J., Zeng, X.B., et al. 2003. The Common Land Model. B Am Meteorol Soc 84(8), 1013-1023.

Devak, M. and Dhanya, C.T. 2017. Sensitivity analysis of hydrological models: review and way forward. J Water Clim Change 8(4), 557-575.

Fernandez-Pato, J., Caviedes-Voullieme, D., et al. 2016. Rainfall/runoff simulation with 2D full shallow water equations: 390 Sensitivity analysis and calibration of infiltration parameters. J Hydrol 536, 496-513.

Fang, Z., H.R. Bogena, et al.. 2015. Spatio-temporal validation of long-term 3D hydrological simulations of a forested catchment using empirical orthogonal functions and wavelet coherence analysis. J. Hydrol. 529, 1754-1767. doi:10.1016/j.jhydrol.2015.08.011.

Fang, Z., H.R. Bogena, et al.. 2016. Scale dependent parameterization of soil hydraulic conductivity in the 3D simulation of hydrological processes in a forested headwater catchment. J. Hydrol. 536, 365–375. doi:10.1016/j.jhydrol.2016.03.020.

Frey, H.C. and Patil, S.R. 2002. Identification and review of sensitivity analysis methods. Risk Anal 22(3), 553-578.

Gebler, S., H.-J. Hendricks Franssen, et al. 2017. High resolution modelling of soil moisture patterns with TerrSysMP: A comparison with sensor network data. J. Hydrol. 547, 309-331.

Hall, J.W., Boyce, S.A., et al. 2009. Sensitivity Analysis for Hydraulic Models. J Hydraul Eng-Asce 135(11), 959-969.

Hersbach, H., Bell, B., et al. 2020. The ERA5 global reanalysis. Quarterly Journal of the Royal Meteorological Society 146(730), 1999-2049.

Göhler, M., Mai, J., and Cuntz, M.: Use of eigendecomposition in a parameter sensitivity analysis of the Community Land Model, Journal of Geophysical Research: Biogeosciences, 118, 904-921, https://doi.org/10.1002/jgrg.20072, 2013.

Jefferson, J.L., Gilbert, J.M., et al. 2015. Active subspaces for sensitivity analysis and dimension reduction of an integrated hydrologic model. Comput Geosci-Uk 83, 127-138.

Jefferson, J.L. and Maxwell, R.M. 2015. Evaluation of simple to complex parameterizations of bare ground evaporation. J Adv Model Earth Sy 7(3), 1075-1092.

Jefferson, J.L., Maxwell, R.M., et al. 2017. Exploring the Sensitivity of Photosynthesis and Stomatal Resistance Parameters in a Land Surface Model. J Hydrometeorol 18(3), 897-915.

Jencso, K.G., McGlynn, B.L., et al. 2010. Hillslope hydrologic connectivity controls riparian groundwater turnover: Implications of catchment structure for riparian buffering and stream water sources. Water Resour Res 46.

Jolly, I.D., McEwan, K.L., et al. 2008. A review of groundwater-surface water interactions in arid/semi-arid wetlands and the consequences of salinity for wetland ecology. Ecohydrology 1(1), 43-58.

Koch, J., Cornelissen, T., et al. 2016. Inter-comparison of three distributed hydrological models with respect to seasonal variability of soil moisture patterns at a small forested catchment. J Hydrol 533, 234-249.

Kollet, S.J. and Maxwell, R.M. 2006. Integrated surface-groundwater flow modeling: A free-surface overland flow boundary condition in a parallel groundwater flow model. Adv Water Resour 29(7), 945-958.

Kollet, S.J. and Maxwell, R.M. 2008a. Capturing the influence of groundwater dynamics on land surface processes using an integrated, distributed watershed model. Water Resour Res 44(2).

Kollet, S.J. and Maxwell, R.M. 2008b. Demonstrating fractal scaling of baseflow residence time distributions using a fully-coupled groundwater and land surface model. Geophys Res Lett 35(7).

Kottek, M., Grieser, J., et al. 2006. World map of the Koppen-Geiger climate classification updated. Meteorol Z 15(3), 259-263.

Linhoss, A., Munoz-Carpena, R., et al. 2013. Hydrologic Modeling, Uncertainty, and Sensitivity in the Okavango Basin: Insights for Scenario Assessment. J Hydrol Eng 18(12), 1767-1778.

Maxwell, R.M. 2013. A terrain-following grid transform and preconditioner for parallel, large-scale, integrated hydrologic modeling. Adv Water Resour 53, 109-117.

Maxwell, R.M., Condon, L.E., et al. 2015. A high-resolution simulation of groundwater and surface water over most of the continental US with the integrated hydrologic model ParFlow v3. Geosci Model Dev 8(3), 923-937.

430 Maxwell, R.M. and Miller, N.L. 2005. Development of a coupled land surface and groundwater model. J Hydrometeorol 6(3), 233-247.

Melsen, L.A. and Guse, B. 2021. Climate change impacts model parameter sensitivity - implications for calibration strategy and model diagnostic evaluation. Hydrol Earth Syst Sc 25(3), 1307-1332.

Morris, M.D. 1991. Factorial Sampling Plans for Preliminary Computational Experiments. Technometrics 33(2), 161-174.

435 Oleson, K.W., Niu, G.Y., et al. 2008. Improvements to the Community Land Model and their impact on the hydrological cycle. J Geophys Res-Biogeo 113(G1).

Pianosi, F., Beven, K., et al. 2016. Sensitivity analysis of environmental models: A systematic review with practical workflow. Environmental Modelling & Software 79, 214-232.

Rihani, J.F., Maxwell, R.M., et al. 2010. Coupling groundwater and land surface processes: Idealized simulations to identify
440 effects of terrain and subsurface heterogeneity on land surface energy fluxes. Water Resour Res 46.

Saltelli, A., Annoni, P., et al. 2010. Variance based sensitivity analysis of model output. Design and estimator for the total sensitivity index. Comput Phys Commun 181(2), 259-270.

Saltelli, A., Tarantola, S., et al. 1999. A quantitative model-independent method for global sensitivity analysis of model output. Technometrics 41(1), 39-56.

445 Schaap, M.G., Leij, F.J., et al. 2001. ROSETTA: a computer program for estimating soil hydraulic parameters with hierarchical pedotransfer functions. J Hydrol 251(3-4), 163-176.

Seck, A., Welty, C., et al. 2015. Spin-up behavior and effects of initial conditions for an integrated hydrologic model. Water Resour Res 51(4), 2188-2210.

Sophocleous, M. 2002. Interactions between groundwater and surface water: the state of the science. Hydrogeol J 10(1), 52-
450 67.

Srivastava, V., Graham, W., et al. 2014. Insights on geologic and vegetative controls over hydrologic behavior of a large complex basin - Global Sensitivity Analysis of an integrated parallel hydrologic model. J Hydrol 519, 2238-2257.

Stein, M. 1987. Large Sample Properties of Simulations Using Latin Hypercube Sampling. Technometrics 29(2), 143-151.

van Griensven, A., Meixner, T., et al. 2006. A global sensitivity analysis tool for the parameters of multi-variable catchment
455 models. J Hydrol 324(1-4), 10-23.

van Genuchten, M.T. 1980. A Closed-Form Equation for Predicting the Hydraulic Conductivity of Unsaturated Soils. Soil Sci Soc Am J 44(5), 892-898.

Wang, A., Solomatine, D.P. 2019. Practical Experience of Sensitivity Analysis: Comparing Six Methods, on Three Hydrological Models, with Three Performance Criteria. Water 11(5).

460 Wood, E. F., Roundy, J. K., et al. 2011. Hyperresolution global land surface modeling: Meeting a grand challenge for monitoring Earth's terrestrial water. Water Resour Res 47.